A Systematic Experimental Approach in Deriving Stator-Winding Heat Transfer

Rafal Wrobel, Sabrina Ayat, Jonathan Godbehere
Department of Electrical & Electronic Engineering, University of Bristol, Bristol, UK,
r.wrobel@bristol.ac.uk, s.ayat@bristol.ac.uk, jg7560@bristol.ac.uk

Abstract—**This work is devoted to providing a more systematic approach to thermal design and analysis of electrical machines with the research focused on heat transfer from the winding body to the stator core pack/machine periphery. The heat transfer from the winding body is notoriously difficult to predict theoretically due to the multi-material composite structure of the stator-winding assembly. Together with numerous manufacture and assembly factors, the heat transfer is usually informed empirically. Further to this, the stator-winding assembly frequently constitutes the main source of power loss within a machine assembly. Both the heat transfer and power loss effects have a significant impact on the machine's overall power output capability.**

A common approach when quantifying the heat transfer across the stator-winding is based on an equivalent thermal resistance. This method provides reliable information regarding the capability of the dissipative heat transfer. However, as the thermal resistance data is related to a particular machine and stator-winding assembly, the results are difficult to transfer and compare across different machine designs. Especially if no supplementary stator-winding construction data is available. Here, a method utilising an equivalent thermal conductance has been proposed to enable data transfer for the alternative machine builds and topologies. This allows for a relatively simple comparison among alternative stator-winding assemblies. Both the experimental and theoretical findings are presented in the paper to illustrate the proposed approach.

Keywords—thermal analysis; thermal design; stator-winding heat transfer; thermal resistance; thermal conductance; electrical machines;

I. INTRODUCTION

It is desirable at the initial design stage of a machine, to be able to make fully informed decisions regarding the winding arrangement and construction. In order to enable low-loss and effective heat extraction. It has been shown in the literature however, that the design process solely based on the theoretical analyses is frequently insufficient, in particular when the thermal design of electrical machines is considered [1]-[14]. This is related to numerous manufacture and assembly factors, which require experience from previous hardware developments if new and unfamiliar machine designs are envisaged. [2]-[13]. A simple transfer of the empirically derived design factors for the alternative machine variants/topologies is usually limited. Consequently, there is a need for an approach enabling transferability of the design factors associated with the stator-winding region.

This investigation considers a class of machine constructions, where the generated heat from the winding body is transferred to the machine periphery by conduction. The existing body of work related with the thermal design and analysis of electrical machines provides various methods of representing and accounting for the stator-winding heat transfer. All these techniques are strongly related with the experimental and/or theoretical methods used [1]-[9]. However, the various existing approaches do not allow for a simple and direct comparison of the heat transfer efficacy between alternative machines and stator-winding designs. In this work, the authors propose an experimental approach of deriving the stator-winding heat transfer, enabling direct assessment and comparison of the design candidates. The method utilises an equivalent thermal conductance as a mean of quantifying the stator-winding heat transfer.

A single stator-winding slot is treated here, to some degree, as a 'black box' with the equivalent thermal properties of the impregnated winding and winding to stator contact to be unknown. The proposed method allows for the resultant/ combined stator-winding thermal properties to be derived in a decoupled manner, i.e. applicable to any heat extraction method from the machine periphery. A number of alternative hardware stator-winding assemblies have been tested and compared. These include complete stator-windings and stator-winding sectors (motorettes) with concentrated and distributed winding topologies and a number of different conductor arrangements, and winding impregnating materials.

A direct assessment of the experimental data collected from thermal tests on the individual hardware exemplars would not be adequate here. To provide a fair comparison, the experimental work has been supplemented with theoretical analyses. Here, the theoretical body of work has been used to derive a set of correction functions, separately for the slot shape and slot size. Both geometrical factors have a significant impact on absolute value of the thermal conductance estimates. The proposed approach enables a simple comparison of thermal heat transfer, from the winding body to the laminated stator core pack, among variety of the stator-winding assemblies.

Also, the results have revealed that the concentrated winding topologies offer significantly better stator-winding dissipative heat transfer, per an equivalent stator slot, as compared with the distributed wound designs. However, when comparing results for the complete stator assembly accounting for the overall slot periphery the difference between the concentrated and distributed wound machines is less prominent. Both the observations are, to a degree, expected considering the analysed

stator-winding arrangements. A more detailed discussion of the research is provided in consecutive sections of the paper.

II. Hardware Exemplars

A number of different stator-winding exemplars has been analysed in the investigation, see Fig. 1. The selected hardware includes the complete stator-winding and stator-winding motorette assemblies with concentrated and distributed winding arrangements. The hardware exemplars have been selected such that a variety of the winding conductor types and constructions is considered. Starting from a single strand of round conductor [4], following with a multi-stranded bundle [15], a compacted type-8 Litz wire [2], a profiled rectangular conductor [16] and compressed multi-stranded coil construction [17].

a) Exemplar I – w/h = 0.67
S_{ca} = 665mm^2

b) Exemplar II – w/h = 0.19
S_{ca} = 219mm^2

c) Exemplar III – w/h = 0.13
S_{ca} = 38mm^2

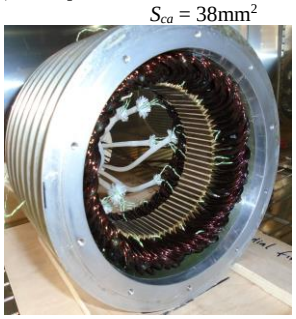

d) Exemplar IV – w/h = 1.13
S_{ca} = 451mm^2

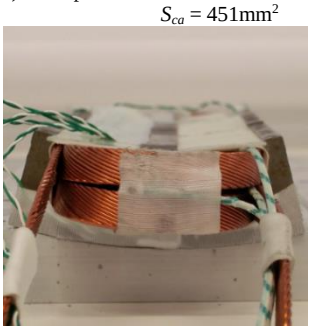

e) Exemplar V – w/h = 0.82
S_{ca} = 537mm^2

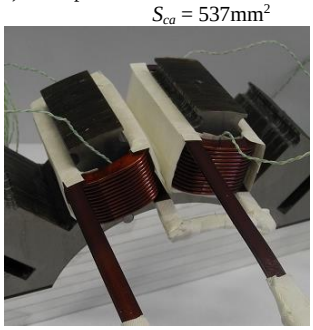

f) Exemplar VI – w/h = 0.89
S_{ca} = 356mm^2

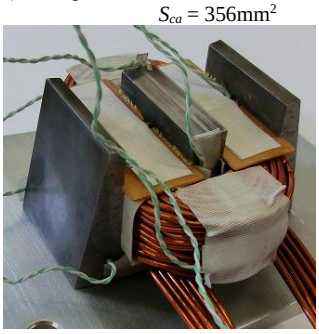

Fig. 1. Analysed hardware exemplars, a) concentrated winding with multi-stranded bundle of round profiled copper conductors, b) distributed winding with multi-stranded bundle of round profiled copper conductors, c) distributed winding with single strand of round aluminium conductor, d) concentrated winding with compacted type-8 Litz wire with copper conductors, e) concentrated winding with edge-wound rectangular profiled copper conductor, f) compressed concentrated winding with multi-stranded bundle of aluminium conductors

TABLE I. Selectecd Data for the Analysed Exemplars

	Exemplar					
	I	II	III	IV	V	VI
a)	10/12	10/36	16/72	28/24	10/12	20/24
b)	1.9	1.9	4.8	1.4	4.9	9.4
c)	0.65	0.43	0.34	0.75	0.67	0.39
d)	Ø0.80	Ø0.67	Ø1.70	7AWG 20/20[1)]	1.50 7.00	Ø1.67
e)	45%	45%	47%	50%	36%	55%
f)	[2)]	[2)]	[3)]	[4)]	[4)]	[4)]
g)	[5)]	[5)]	[6)]	[5)]	[5)]	[5)]
h)	H	H	H	H	H	H

a) Number of poles/slots;
b) Outer diameter to active length ratio;
c) Active winding length to total winding length; $l_a/(l_a+l_e)$; l_a – winding active length; l_e – end-winding length;
d) Conductor gauge [mm]; [1)] New England Wire Technologies;
e) Slot fill factor;
f) Impregnating varnish; [2)] Ultimeg 2000/380 by AEV; [3)] ELAN-protect UP142 by Elantas; [4)] Elmotherm 073-1010 by Elantas;
g) Slot linear; [5)] Nomex 410 by Dupont; [6)] ThermaVolt by 3M;
h) Wire insulation/enamel class; (class H, 180°C);

Table I lists selected data for the analysed stator-winding exemplars including the electrical insulation system type/class and electrical wire details. All the stator-winding assemblies use the same slot liner material and are varnish impregnated. A more comprehensive information regarding the machine/stator-winding constructions is provided in the referred to earlier literature references. Fig. 1 also provides, the averaged per slot width to height aspect ratio (w/h) and per slot active cross-section area (S_{ca}) data for the analysed hardware. Both the geometrical parameters have significant impact on effectiveness of the dissipative heat transfer from the winding body to the core pack and are used to adjust the measured thermal data, to provide

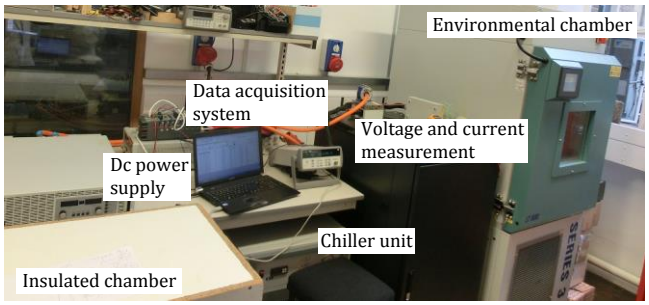

Fig. 2. Experimental setup for thermal testing

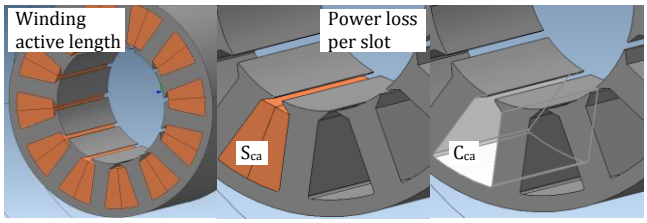

Fig. 3. Schematic procedure of deriving equivalent stator-winding thermal resistance and conductance

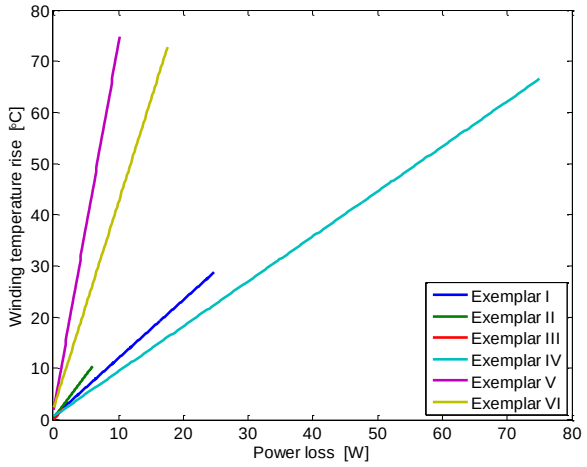

Fig. 4. Winding temperature rise above core vs. per slot power loss; All the measured quantities are averaged and refer here to the active length region

a fair and clear comparison, details of which are discussed in the following sections of the paper.

III. Experimental Setup And Testing Procedure

To derive the stator-winding heat transfer, the standard steady state thermal tests with dc winding excitation have been employed here [2]-[4]. For the complete stator-winding testing, the housed machine assembly together with end caps is placed in an environmental chamber and tested at a controlled temperature. The motorette experimentation has been performed using an insulated chamber, where the stator-winding section under test is mounted on a liquid cooled, temperature controlled cold plate [2]. Fig. 2 presents the experimental setup with the constituent components/ instruments indicated. Both testing methods encourage a well defined conductive heat transfer path from the winding heat source, into the heat sink or environment, across the stator core pack. For the hardware with multiple phases stator-winding arrangement, i.e. complete stator winding assembly, the per slot dc power loss is identical for all stator slots. This is realised by appropriately configuring the winding coils and/or phases, e.g. series or parallel connection of the individual winding phases.

During the tests, the measured temperature and input dc power data is recorded. The temperatures are measured within the winding active and end regions, and the stator core pack. The collected winding and core temperatures for the stator-winding active region are averaged and together with power loss data per slot active length are used to derive the equivalent stator-winding thermal resistance and conductance.

$$R_e = \frac{d\Delta T}{dP} \quad , \qquad (1)$$

$$h_e = \frac{1}{R_e C_{ca}} \quad , \qquad (2)$$

where ΔT is the averaged temperature difference between the winding and core, P is the power loss per slot active length and C_{ca} is the winding to stator surface area, across which the heat is dissipated from the winding body into the laminated stator core pack.

Fig. 3 schematically illustrates the procedure of deriving both the quantities, whereas (1) and (2) provides the mathematical description. It is important to remind that both the equivalent stator-winding thermal resistance and conductance are derived based on data gathered for a single stator slot over the winding active length. Fig. 4 presents raw data from the measurements showing the characteristic linear variation of the winding temperature rise with input/generated power loss. In the analysis, it has been assumed that the heat flux from/to end-winding is negligible and does not affect the overall results. However, this assumption might not be applicable in all cases, and the end-winding heat transfer effects need to be accounted for. The end-winding heat transfer effects are discussed in the next section the paper.

IV. Theoretical Analysis

A. Slot Geometry Correction Functions

When comparing the conductive heat transfer across the winding body into the stator core and machine periphery, two slot geometrical factors need to be accounted for. The first one is related with the slot shape and is defined by the averaged w/h ratio, whereas the second one is given by the per slot active cross-section area S_{ca}. Both factors would ideally need to be the same, for the individual stator-winding assemblies, to make the comparison meaningful. Clearly, this condition is difficult to be satisfied in the majority of practical cases, including the selected hardware exemplars.

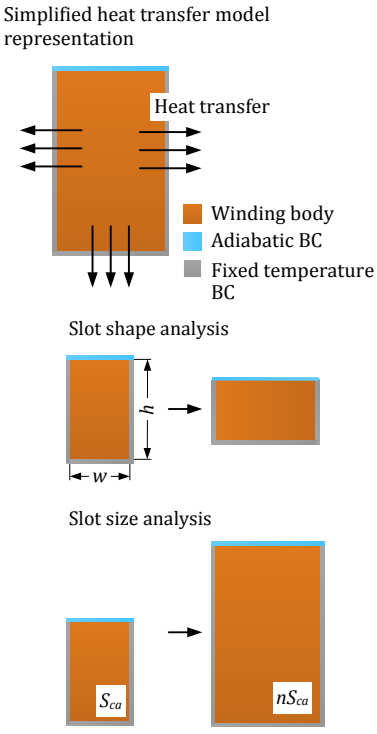

Fig. 5. Simplified FE 2D thermal model representation for derivation of the slot shape and slot size correcting functions

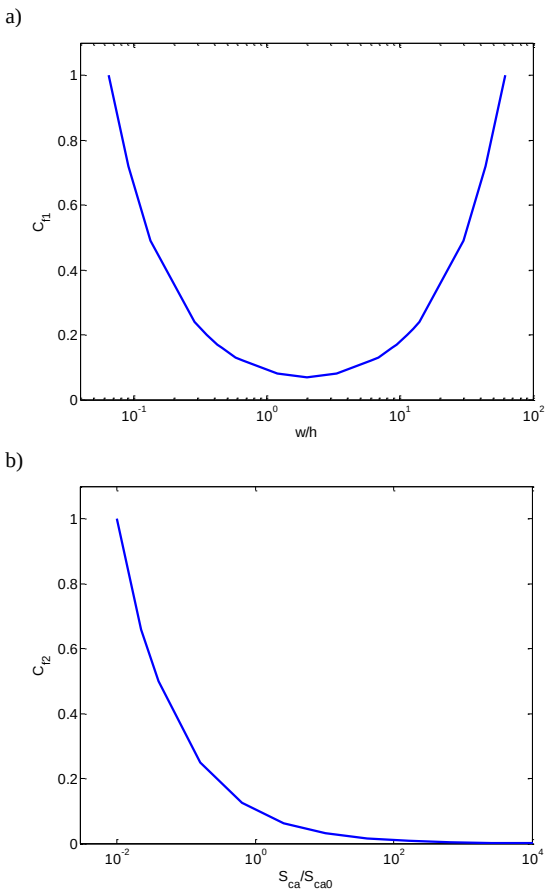

Fig. 6. Correcting functions for a) slot shape C_{f1} vs. w/h, b) slot size C_{f2} vs. S_{ca}/S_{ca0}

To enable an unconstrained comparison, two correcting functions have been introduced, the shape function ($C_{f1}(w/h)$) and the size function ($C_{f2}(S_{ca}/S_{ca0})$), where S_{ca0} is equal to 10^3mm^2 in this investigation.

The correcting functions have been derived theoretically from thermal analyses and are used to adjust the measured data from the thermal tests. Fig. 5 shows a schematic thermal model representation together with the boundary conditions (BCs), which has been used in derivation of the slot shape and slot size correcting functions. A two-dimensional (2D) thermal finite element analysis (FEA) has been used here. In this simplified analysis, the laminated stator core pack assembly is represented by a fixed temperature boundary condition emulating the stator core at an average temperature. The heat transfer from the stator slot opening is assumed to be negligible. Also, the stator-winding slot is represented here, as a 'black box' region defined with a composite thermal material property. The dc power loss generated within the winding region is assumed to be homogenously distributed. It is important to note that absolute values of thermal conductance derived from the FEAs are strongly dependent on the initial assumptions regarding the BCs and thermal material properties. However, as in this analysis the functional trends are of consideration only, the BCs and thermal material properties are of lesser importance, i.e. the functional trends are independent on boundary and material settings.

For the slot shape analysis, the w/h ratio is adjusted, such that the slot contour, through which the heat is dissipated from the winding body to the stator core pack, remains unchanged. It is important to remember that the heat transfer through the slot-opening was assumed to be negligibly small, compared with the main stator-winding heat transfer path. The slot size analysis assumes a fixed w/h ratio for a range of selected slot cross-sections. Both the correcting functions have been individually obtained following the procedure employed in the hardware testing. The calculated normalised values of thermal conductance, from the thermal FEAs, define the correcting functions C_{f1} and C_{f2}, Fig. 6. The maximum value of the thermal conductance has been used to normalise the data separately for the slot shape and slot size functions. It is important to note that the correcting functions C_{f1} and C_{f2} are independent of the slot size and slot shape respectively, initially assumed in the thermal analysis.

When analysing variation of the functions, the expected trends in stator-winding heat transfer are observed. The slot shape function suggests, that the 'narrow-deep' and 'wide-shallow' slot geometries have similar capabilities of conducting heat from the winding body, Fig. 6a). It is interesting to note that the function is symmetrical, with the symmetry point for $w/h = 2$. This corresponds with the largest slot cross-section area among analysed w/h ratios for a fixed length of the winding-to-slot contour. The theoretical symmetry, results from the initial assumption regarding negligible heat transfer from the slot opening region (adiabatic BC), Fig. 5. The size function indicates that the 'large' slots have poorer dissipative heat transfer capabilities as compared with the 'small' slots. This is a consequence of the winding thermal resistance to be larger for the 'large' slots as compared with the 'small' equivalents.

The measured values of thermal conductance are adjusted for slot shape and slot size using the following formulae,

$$h_e(w/h)_i = h_e(w/h)_m \frac{C_{f1}((w/h)_i)}{C_{f1}((w/h)_m)} \quad , (3)$$

$$h_e(S_{ca}/S_{ca0})_i = h_e(S_{ca}/S_{ca0})_m \frac{C_{f2}((S_{ca}/S_{ca0})_i)}{C_{f2}((S_{ca}/S_{ca0})_m)} \quad , (4)$$

where subscripts i and m refer to adjusted for and measured at w/h or S_{ca}/S_{ca0} factors respectively. Values of the correcting functions C_{f1} and C_{f2} can be found at any w/h or S_{ca}/S_{ca0} by interpolating the FE derived data or using curve fit. (5) and (6) provide mathematical description for C_{f1} and C_{f2} functions,

$$C_{f1}(x) = p_{11}x^4 + p_{12}x^3 + p_{13}x^2 + p_{14}x + p_{15} \quad , (5)$$

$$x = \log_{10}(w/h)$$
$$p_{11} = 0.1255$$
$$p_{12} = -0.1514$$
$$p_{13} = 0.2007$$
$$p_{14} = -0.09264$$
$$p_{15} = 0.09307$$

$$C_{f2}(x) = p_{21}e^{(p_{22}x)} \quad , \quad (6)$$

$$x = \log_{10}(S_{ca}/S_{ca0})$$
$$p_{21} = 0.09925$$
$$p_{22} = -1.154$$

B. *End-Winding Heat Transfer Effects*

The above analysis assumes that heat transfer associated with the end-winding region is negligible. In an ideal case, the averaged per region temperature difference between the active and end winding would be equal to zero, i.e. no heat transfer between the domains. In practice, the measured temperature difference is usually non zero. The averaged winding temperature over the entire winding length can be estimated relatively easy from measurements of variation in the winding dc resistance. However, the averaged per winding region temperature measurement is more challenging due to the frequently limited use of thermal sensors. Consequently, there is a degree of uncertainty associated with the per region temperature measurements if no information about location of the thermal sensors is available.

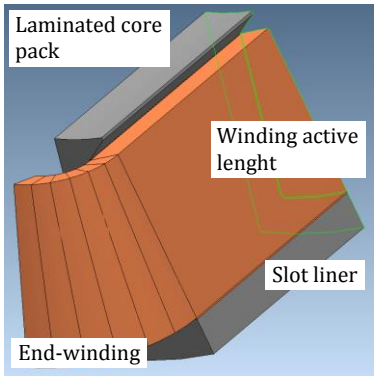

Fig. 7. 3D FE thermal model representation for analysis of the end-winding heat transfer effects – Exemplar I

In this investigation, to illustrate impact of the end-winding heat transfer effects on the thermal conductance estimates, a number of three-dimensional (3D) FEAs have been carried out. The Exemplar I has been selected here as a case study. Fig. 7 presents 3D thermal model representation of an individual stator-winding segment with all the assembly regions indicated. A one quarter of the complete segment with appropriate BCs has been modelled. It is assumed, that dc power loss generated in the winding body is evacuated from the motorette assembly mainly via stator back iron surface. This is modelled by setting a fixed temperature BC on the stator back iron outer surface in the FE thermal model. The remaining surfaces of the model are set with adiabatic BC with the exception of the end-winding region. The end-winding dissipative heat transfer is adjusted here to achieve different heat transfer between the active length and end-winding regions. The assumed material equivalent properties account for thermal anisotropy [18], [19]. As the temperature difference between the winding regions depends on the winding power loss, the volumetric power loss generated in the winding region is the same for all the analysed variants, 10^6W/m^3.

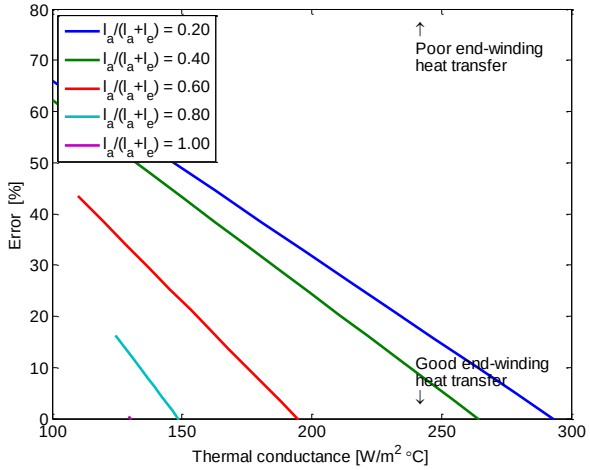

Fig. 8. Error of estimating thermal conductance vs. thermal conductance for 'good' stator-winding heat transfer – Exemplar I; l_a – winding active length; l_e – end-winding length

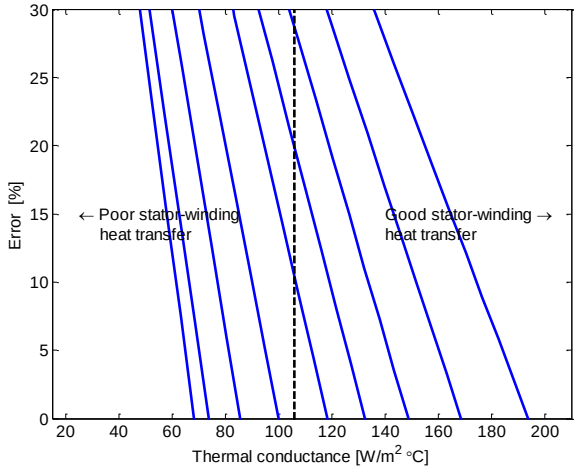

Fig. 9. Error of estimating thermal conductance vs. thermal conductance – Exemplar I; $l_a/(l_a+l_e)$ = 0.65

Fig. 8 shows a variation in error of estimating thermal conductance versus thermal conductance, h_e. The zero heat transfer between the end and active length winding regions is assumed here as a baseline for calculating the error. It is important to note that the upper limit of the calculated error is representative of poor heat extraction from the end-winding, e.g. end-winding is perfectly insulated, i.e. adiabatic insulation. Consequently, heat generated in the end-winding is transferred from the end to active length of the winding. This results in the thermal conductance predictions to be underestimated due to temperature of the winding active length to be higher than for the baseline case with zero heat transfer. For the machine designs with active heat extraction from the end-winding region, a reversed situation is expected. A portion of heat generated in the active length region would be extracted via end-winding resulting in a negative error of estimating thermal conductance, i.e. thermal conductance is overestimated.

Furthermore, the results indicate that the end-winding relative length has a significant impact on estimates of the thermal conductance, which is evident when comparing results for the machines with different ratios of active length to overall winding length, e.g. thermal conductance at zero error. It is important to note that for the purpose of this illustration, 'good' stator-winding heat transfer with perfect contact thermal resistance has been assumed. However, the initial assumptions regarding 'goodness' of the stator-winding heat transfer path have a prominent impact on the overall heat transfer effects […]. Fig. 9 presents again the variation in error of estimating thermal conductance versus thermal conductance, h_e. This time however, the effect of initial assumptions regarding the stator-winding heat transfer 'goodness' is illustrated. Each of the graphs shown in Fig. 8 represents a model with different stator-winding heat transfer 'goodness'. The results indicate ambiguity related with definition of the thermal model, e.g. there are numerous models providing the same value of thermal conductance, see dashed line in Fig. 8. Clearly, a model calibration using detailed thermal data would need be used to resolve this issue. This however, is beyond the scope of this work.

It is evident that the end-winding effects are difficult to account for in a generic and simple manner. In particular, the end-winding heat transfer effects are challenging to be derived experimentally and/or theoretically. Considering a large variety of the analysed end-winding designs, at this stage of research, no correction for heat transfer from/to the end-winding was used as such. However, based on the initial findings, an attempt was made to account for the end-winding relative length. Fig. 10 shows variation of the proposed correcting function for the relative end winging length, C_{f3}. Similarly, as for the slot shape, and slot size correcting functions, C_{f1} and C_{f2}, C_{f3}, has been derived from variation of thermal conductance, h_e. Here, zero heat transfer between end and active length winding regions was considered, Fig. 8. The calculated data was then normalised to the maximum value of the thermal conductance data set. Consequently, the functional variation is independent on the stator-winding heat transfer 'goodness'.

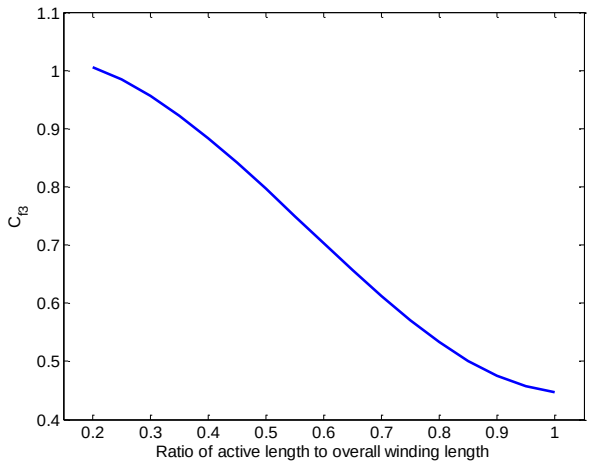

Fig. 10. Correcting functions for end-winding relative length C_{f3}

It is important to note that C_{f3} is specific to the particular winding design, Exemplar I, and might not be applicable to any end-winding/winding topology. In this investigation however, it was assumed that C_{f3} applies for all the analysed stator-winding exemplars.

$$h_e\big(l_a/(l_a+l_e)\big)_i = h_e\big(l_a/(l_a+l_e)\big)_m \frac{C_{f3}(l_a/(l_a+l_e)_i)}{C_{f3}(l_a/(l_a+l_e)_m)} \quad , (7)$$

$$C_{f3}(x) = p_{31}x^3 + p_{32}x^2 + p_{33}x + p_{34} \quad , (8)$$

$$x = l_a/(l_a+l_e)$$
$$p_{31} = 1.4827$$
$$p_{32} = -2.5250$$
$$p_{33} = 0.4939$$
$$p_{34} = 0.9951$$

(7) and (8) provide mathematical description for the he adjustment with relative length of the end-winding. The nomenclature used in (7) and (8) is equivalent to that described in the previous section.

V. Results

TABLE II. Stator-Winding Thermal Resistance and Conductance Data

	Exemplar					
	I	II	III	IV	V	VI
a)	1.14	1.68	1.50	0.88	7.15	4.01
b)	106.62	85.76	524.53	92.62	80.59	123.92
c)	109.86	12.58	22.20	133.19	88.97	82.54
d)	0.82	0.09	0.17	1.00	0.67	0.62
e)	112.60	68.41	245.41	139.03	80.16	103.43
f)	0.45	0.28	1.00	0.57	0.32	0.42

a) Thermal resistance, R_e [°C/W];
b) Thermal conductance, h_e [W/m^2 °C];
c) Equivalent thermal conductance, h_{e12} [W/m^2 °C] for w/h = 0.7, S_{ca}/S_{ca0} = 0.5 and $l_a/(l_a+l_e)$ = 0.7
d) Ratio of h_{e12} to h_{e12max};
e) Equivalent thermal conductance, h_{e13} [W/m^2 °C] for identical qS_{ca}, $l_a/(l_a+l_e)$ = 0.7and w/h as in Fig. 1;
f) Ratio of h_{e13} to h_{e13max};

Table III lists a complete set of results from the analysis. When examining the results it is evident that the use of equivalent thermal resistance, R_e, is limited for the studies comparing different stator-winding designs and/or topologies. Here, the results suggest that Exemplar V has the stator-winding heat transfer capability significantly poorer than other analysed hardware. However, when comparing the equivalent thermal conductance, h_e, derived directly from the measurements, the difference among the design variants is less prominent as compared with the R_e data. Here, Exemplar III has the best conductive path from the winding to the stator/machine periphery. Clearly, the use of thermal conductance allows one

to decouple the measured thermal data from a particular stator-winding topology, which is evidenced in (1). It is important to remember that the equivalent thermal conductance referred to in this work defines the per slot conductive heat transfer.

It has been shown earlier that the conductive heat transfer from the winding body is affected by shape and size of the stator slot, in which the winding is placed and the end-winding relative length. Consequently, to compare the per slot heat transfer capabilities, a correction for these three factors needs to be used. Here, the slot shape, size and relative end-winding length correcting functions, C_{f1}, C_{f2} and C_{f3} have been employed to derive h_{e12}. For the purpose of the comparison, it has been assumed that $w/h = 0.7$, $S_{ca}/S_{ca0} = 0.5$ and $l_a/(l_a+l_e) = 0.7$. The corrected data indicates that the concentrated-wound winding topologies have significantly better per slot conductive heat transfer as compared with the distributed-wound winding designs. This is expected outcome as the distributed windings have usually poorer conductor fill factor and build quality.

However, as distributed windings have more slots than concentrated topologies, the poorer per-slot conductive heat transfer is compensated for. This, together with a smaller in size and elongated narrow slot shape, further improves the conductive heat evacuation from the winding body. The h_{e13} quantity illustrates this effect, where the overall slot cross-section for a complete machine case study is identical for all the analysed exemplars. The w/h ratio for the individual stator-winding designs remains the same as listed in Fig. 1, and the relative end-winding length is set to 0.7. Here, the results suggest that the difference between the concentrated and distributed windings in less prominent. The corrected data for exemplars I and II is particularly interesting as both the laminated stator core packs have an identical mechanical envelope and overall slot cross sectional area. Also, the winding construction and materials used are similar in both cases. However, despite the fact that the winding to stator contact area, C_{ca}, is 2.5 times larger for exemplar II than exemplar I, the equivalent thermal conductance e) is approximately 40% larger for exemplar I than exemplar II. This is attributed to a better build quality, with an improved stator-winding heat transfer and lesser end-winding contribution for exemplar I as compared with exemplar II.

In general, the stator-winding conductive heat transfer for exemplar III stands out among the analysed hardware. This results predominantly from the well-controlled winding construction and use of insulating system with improved thermal properties. Also, exemplar III has the smallest active length to overall winding length ratio, $l_a/(l_a+l_e) = 0.34$, consequently the overall impact of the end-winding here is the largest. As it has been mentioned earlier, the employed correction factor for the end-winding might not be applicable for all of the analysed stator-winding exemplars. A more detailed analysis is needed to provide a more comprehensive insight into the end-winding heat transfer effects. This however, is beyond the scope of this paper and will be investigated by the authors in the future work.

VI. Conclusions

This paper proposes a systematic approach to comparing the conductive heat transfer for various stator-winding topologies. Building upon thermal analysis of the winding and slot region, as an alternative to complete machine hardware testing. A time effective comparison and initial design choices regarding the stator-winding can be made using the technique if supported by an appropriate experimental data repository. Furthermore, the proposed method can be used in calibration of the stator-winding region for the complete thermal models, which is essential in thermal design and deriving operating envelopes and/or working cycles.

It is important to remember, that the aim of this investigation was to provide a simple and computationally inexpensive approach for assessing the stator-winding heat transfer without any need for supplementary thermal analysis. The proposed method was built upon experimentally derived data from thermal tests on a variety of stator-winding hardware samples, and observations from simplified thermal analyses. Both these factors have a limiting impact on applicability of the proposed approach. The technique provides estimates for the equivalent thermal conductance rather than precise predictions, whereas a finite collection of thermal data does not account for all possible or required combinations of component and materials. Nevertheless, the estimates are beneficial at initial stage of the machine design process, even when limited to a fixed number of design choices.

Future work will look to develop and experimentally validate the design methodology. This will include further investigation into the end-winding contribution to the stator-winding heat transfer and refining the thermal testing approach. These however, will be investigated by the authors in the future research.

Acknowledgment

The research presented in this paper has been supported with funding from the UK Engineering and Physical Science Research Council, and from the EU under the ADEPT project (FP7 ITN 607361). The authors wish to thank Infolytica Europe for providing the software used in this research.

References

[1] A. Boglietti, A. Cavagnino, D. Staton, "Determination of Critical Parameters in Electrical Machine Thermal Models," *IEEE Transactions on Industry Applications*, Vol. 44, No. 4, pp. 1150-1159, July/August 2008.

[2] R. Wrobel, S. J. Williamson, J. D. Booker, P. H. Mellor, "Characterising the 'in situ' Thermal Behaviour of Selected Electrical Machine Insulation and Impregnation Materials," *IEEE Transitions on Industry Applications*, Vol. 52, No. 6, pp. 4678-4687, November/December 2016.

[3] S. Ayat, R. Wrobel, J. Goss, D. Drury, "Experimental Calibration in Thermal Analysis of PM Electrical Machines," *IEEE Energy Conversion Congress and Exposition, (ECCE2016)*, pp. 1-7, 2016.

[4] J. Godbehere, R. Wrobel, D. Drury, P. H. Mellor, "Experimentally Calibrated Thermal Stator Modelling of AC Machines for Short-Duty Transient Operation," *International Conference on Electrical Machines (ICEM 2016)*, pp. 1721-1727, 2016.

[5] M. Tosetti, P. Maggiore, A. Cavagniono, S. Vaschetto, "Conjugate Heat Transfer Analysis of Integrated Brushless Generators for More Electric

Engines," *IEEE Transactions on Industry Applications*, Vol. 50, No. 4, pp. 2467-2475, July/August 2014,.

[6] A. Boglietti, E. Carpaneto, M. Cossale, S. Vaschetto, T. Dutra, "Thermal Conductivity Evaluation of Fractional-Slot Concentrated Winding Machines," *IEEE Energy Conversion Congress and Exposition, (ECCE2016)*, pp. 1-7, 2016.

[7] A. Boglietti, E. Carpaneto, M. Cossale, S. Vaschetto, M. Popescu, D. Staton, "Stator winding thermal conductivity evaluation: An industrial production assessment," *IEEE Energy Conversion Congress and Exposition, (ECCE2015)*, pp. 4865-4871, 2015.

[8] J. Baker, R. Wrobel, D. Drury. P. Mellor, "A Methodology for Predicting the Thermal Behaviour of Modular-Wound Electrical Machines", *IEEE Energy Conversion and Exposition (ECCE*), pp. 5176-5183, Pittsburg, 2014.

[9] S. Ayat, R. Wrobel, J. Goss, D. Drury, "Experiment Informed Methodology for Thermal Design of PM Machines", *Eleventh International Conference on Ecological Vehicles and Renewable Energies (EVER*), Monaco, April 2016.

[10] R. Wrobel, P. H. Mellor, N. McNeill, D. A. Staton, "Thermal Performance of an Open-Slot Modular-Wound Machine with External Rotor," IEEE Transactions on Energy Conv., vol. 25, no. 2, pp. 403- 411, June 2010.

[11] R. Wrobel, S.J. Williamson, N. Simpson, S. Ayat, J. Yon, P.H. Mellor, "Impact of slot shape on loss and thermal behaviour of open-slot modular stator windings", *Energy Conversion Congress and Exposition (ECCE)*, pp. 4433-4440, Montreal, 2015.

[12] N. Simpson, R. Wrobel, P. H. Mellor, "A Multiphysics Design Methodology Applied to a High-Force-Density Short-Duty Linear Actuator," *IEEE Transactions on Industry Applications*, Vol. 52, No. 4, pp. 2919-2929, July/August 2016.

[13] F. Márquez-Fernández, J. H. Potgieter., A. Fraser, m. McCulloch, "Thermal management in a high speed switched reluctance machine for traction applications," *IET International Conference on Power Electronics, Machines and Drives (PEMD 2016)*, pp. 6-12, 2016.

[14] S. Y. Goh, J. Wale, D. Greenwood. "Thermal analysis for stator slot of permanent magnet machine." *XXII International Conference on Electrical Machines (ICEM)*, 2016. Lausanne, 2016.

[15] J. Goss, M. Popescu, D. Staton, R. Wrobel, J. Yon P. Mellor, "A comparison between maximum torque/ampere and maximum efficiency control strategies in IPM synchronous machines," *IEEE Energy Conversion Congress and Exposition, (ECCE2014)*, pp. 2403- 2410, 2014.

[16] R. Wrobel, D. Staton, R. Lock, J. Booker, D. Drury, "Winding Design for Minimum Power Loss and Low-Cost Manufacture in Application to Fixed-Speed PM Generator," *IEEE Transactions on Industry Applications*, Vol. 51, No. 5, pp. 3773-3782, September/October 2015.

[17] R. Wrobel, N. Simpson, P. Mellor, J. Goss, D. Staton, "Design of a Brushless PM Starter-Generator for Low-Cost Manufacture a High-Aspect-Ratio," *IEEE Transactions on Industry Applications*, (early access article).

[18] S. Ayat, R. Wrobel, J. Goss, D. Drury, "Estimation of Equivalent Thermal Conductivity for Impregnated Electrical Windings Formed from Profiled Rectangular Conductors", in *8th IET International Conference on Power Electronics, Machines and Drives (PEMD*), Glasgow, April 2016.

[19] N. Simpson, R. Wrobel, P. H. Mellor, "Estimation of Equivalent Thermal Parameters of Impregnated Electrical Windings," *IEEE Transactions on Industry Application*, vol. 49, no. 6, pp. 2505-2515, Nov. 2013.